SLAB-COUPLED OPTICAL WAVEGUIDE (SCOW) OPTOELECTRONIC OSCILLATOR (OEO) SYSTEMS

W. Loh[1,2], S. Yegnanarayanan[1], J. J. Plant[1], J. Klamkin[1], S. Madison[1], F. J. O'Donnell[1], R. J. Ram[2], and P. W. Juodawlkis[1]
[1]Lincoln Laboratory, Massachusetts Institute of Technology
Lexington, MA 02420
[2]Massachusetts Institute of Technology
Cambridge, MA 02139
Tel: 781-981-3887
E-mail: *William.Loh@ll.mit.edu*

Abstract

We report on optoelectronic oscillator (OEO) and coupled optoelectronic oscillator (COEO) systems demonstrated using slab-coupled optical waveguide (SCOW) components for generation of low-noise microwave signals. The OEO employs a high-power, low-noise, narrow linewidth SCOW external cavity laser (SCOWECL) as the optical source, and the COEO uses a low noise SCOW amplifier (SCOWA). High-power, low-noise sources are beneficial for pristine signal generation as the relative intensity noise (RIN) of the optical signal limits the phase-noise of the derived microwave tone. The OEO configuration uses a variable confinement SCOW photodiode (VC-SCOWPD) for signal conversion into the microwave, while initial demonstrations of the SCOW-COEO have used a commercial high-power photodiode. The combination of a high-power SCOWECL and high-power VC-SCOWPD enable the SCOW-OEO to reach oscillation without the use of RF amplification. Using 1.5 km of delay, an OEO operating at 3-GHz carrier frequency demonstrated a phase-noise of -143 dBc/Hz at 10 kHz offset. The SCOW-OEO performance is primarily limited by amplitude-phase noise conversion processes in the photodiode. We also describe measurements on a preliminary 10-GHz SCOW-COEO employing 250 m of delay. The SCOW-COEO exhibited a phase-noise of -134 dBc/Hz at 10 kHz offset frequency with sidemode levels <-127 dBc/Hz.

INTRODUCTION

High performance microwave oscillators are important as stable local oscillators for many applications in radar and GPS and as low phase-noise clocks in communication systems. Most microwave oscillators degrade in performance at higher frequencies due to the increase in signal attenuation during propagation in the resonator **[1]**. Frequency multiplication can theoretically be used to scale the RF tone to any frequency, but the phase-noise of the multiplied signal degrades by 6 dB for every doubling of the oscillation frequency. The optoelectronic oscillator (OEO) is one technique that can potentially be used to generate a microwave signal having low phase-noise that is independent of the RF carrier frequency **[2,3]**.

The basic principle of operation for an OEO involves modulating an RF envelope onto an optical carrier and recovering the microwave signal as a beat tone on the photodiode. The loss due to propagation through fiber is low (~0.2 dB/km at 1.55 μm) allowing for long delay resonators to be achieved with negligible added system loss. The phase-noise operation of an OEO is in principle independent of

frequency as long as the performance of the components in the system (modulator, photodiode, RF filter, RF amplifier, etc.) can be maintained at the higher operating frequencies. Other notable advantages of the OEO are its light weight, immunity to electromagnetic interference, and capability of generating references in both the optical and electrical domains **[2]**. The delay time of the oscillator is critical to reducing phase-noise as doubling the delay reduces close-in phase-noise by 6 dB. The disadvantage of a long-delay oscillator is that the resonance modes satisfying the 2π roundtrip phase condition will be spaced closely in frequency. Typical OEOs exhibit multimode oscillation that can be somewhat suppressed using dual-loop configurations at the cost of complexity and reduced cavity Q **[4]**. Even with these techniques, the OEO sidemodes are still relatively large (-120 dBc/Hz to -100 dBc/Hz), although more complicated injection-locked OEO systems can also be devised to provide sidemode (<-145 dBc/Hz) **[5]**. We have previously demonstrated a single-loop amplifier-free low-noise SCOW-OEO operating at 3 GHz with significantly reduced sidemode spurs **[6]**. The measured phase-noise performance of the oscillator was limited by the noise floor of the phase-noise measurement system used (Agilent E5052B Signal-Source Analyzer (SSA)). In the first section of this paper, we will describe our work using a photonic delay-line system to measure the phase-noise performance of the SCOW-OEO **[7]**.

The coupled optoelectronic oscillator (COEO) is another technique that may be used for suppressing oscillating sidemodes **[8]**. In the second section of the paper, we describe our demonstration of a SCOW coupled optoelectronic oscillator (SCOW-COEO). The COEO is similar to the OEO except that the RF oscillation is driven by a modelocked laser instead of a modulated continuous wave laser. Structurally, the COEO is no different from a regenerative modelocked laser (RML), and many of the principles of regenerative modelocking can be applied to the operation of the COEO **[9]**. The main difference between the RML and the COEO is that the RML primarily focuses on optimization of the optical pulses, while the COEO emphasizes optimization of phase-noise. The optical and RF loops in a COEO form two coupled-cavities, which leads to a complex interaction between the modes of each cavity. The dynamics between the two loops lead to the 'Q-enhancement' of the COEO phase-noise and the suppression of sidemodes by the Vernier effect **[8,10]**. We will show the performance of our 10 GHz COEO containing a novel high-power SCOW amplifier (SCOWA) gain medium.

SLAB-COUPLED OPTICAL WAVEGUIDE OPTOELECTRONIC OSCILLATOR

The SCOW-OEO is similar in configuration to typical OEOs but with high-power SCOW components (SCOW external cavity laser (SCOWECL) and variable confinement SCOW photodiode (VC-SCOWPD)) in place of existing low-power laser and photodiode devices **[11,12]**. This section details the system used for demonstration of the SCOW-OEO.

SCOW-OEO CONFIGURATION

A schematic of our SCOW-OEO system is shown in Figure 1. The laser signal of a SCOWECL operating at 1550 nm with ~300 mW output power and low relative intensity noise (RIN) is sent to a lithium niobate electro-optic modulator (EOM) with V_π = 2.8 V, *loss* = 2.3 dB and >20 dB extinction ratio. One output port of the EOM is monitored on an optical power meter, while the second port is sent to a fiber-stretcher which phase modulates the signal at 60 kHz. The phase modulation suppresses the stimulated Brillouin scattering (SBS) fiber nonlinearity by spreading the power across a large range of frequencies thereby reducing the amount of power that is phase matched within the SBS bandwidth**[13,14]**. The

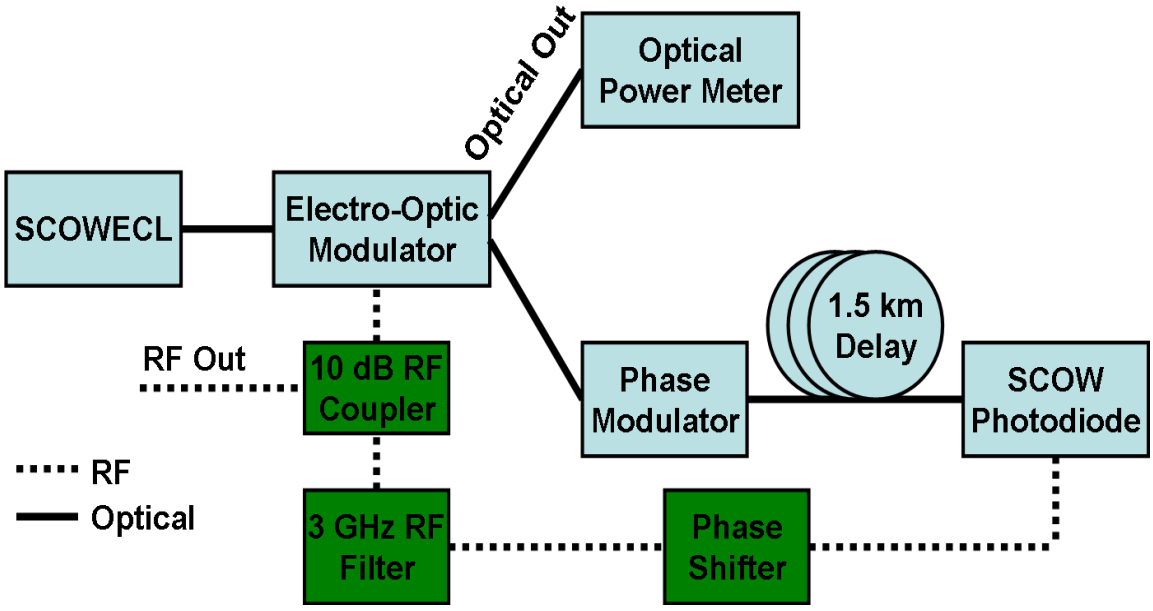

Figure 1. Schematic of the SCOW-OEO configuration.

60 kHz frequency is limited by the modulation speed of the piezo fiber-stretcher. The fiber-stretcher used in our demonstration exhibits ~0.5 dB insertion loss.

In our demonstration of a SCOW-OEO, we employ 1.5 km of single-mode (SMF-28) fiber delay. With phase modulation at 60 kHz, the Brillouin scattering nonlinearity is not suppressed for fiber lengths much larger than 1.5 km. Phase modulation beyond 1 MHz rates are required to significantly suppress SBS for longer fiber delays. The delayed optical signal is sent to a high power VC-SCOWPD exhibiting 3.8 GHz bandwidth, 1 A/W responsivity, and ~38 mA saturation photocurrent **[12]**. The photodiode converts any optical beat signal within its bandwidth into a microwave tone at the difference frequency of the beating. This includes the envelope of the RF modulation, which will be converted to a microwave tone at the OEO oscillation frequency.

The electrical signal is first sent to a manual-control phase shifter (~0.7 dB insertion loss) and then to a 3-GHz dielectric RF filter. The filter exhibits ~2.5 MHz bandwidth and ~1.5 dB insertion loss. The output of the filter is sent to a 10-dB RF coupler with ~0.1 dB added insertion loss. The -10 dB tap of the RF coupler is the useful output of SCOW-OEO, while the remainder of the power is redirected to the RF port of the EOM to achieve self-oscillation.

SCOW-OEO Environmental Isolation System

The components of the SCOW-OEO were housed in two separate isolation boxes in order to isolate the vibration-sensitive elements from external vibration and thermal environmental noise. The most important components to stabilize are the high-Q fiber delay and microwave filter. Both of these elements were housed in a custom designed isolation box illustrated in Figure 2. The box also contains the bias tee for driving the photodiode, a turn-key RF phase shifter, and a piezo fiber-stretcher phase

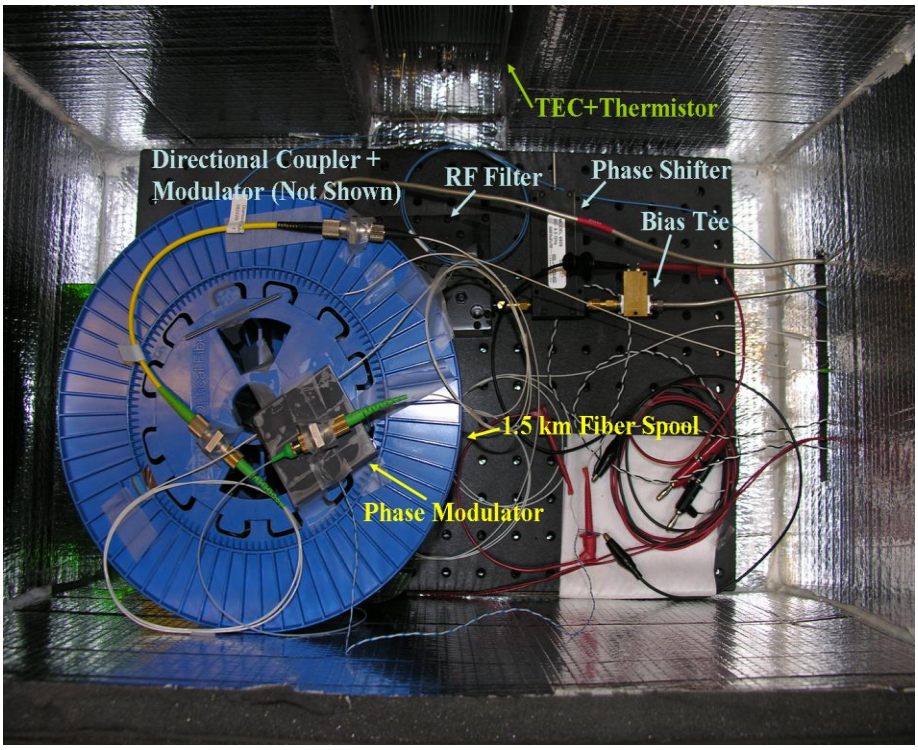

Figure 2. SCOW-OEO passive component isolation box.

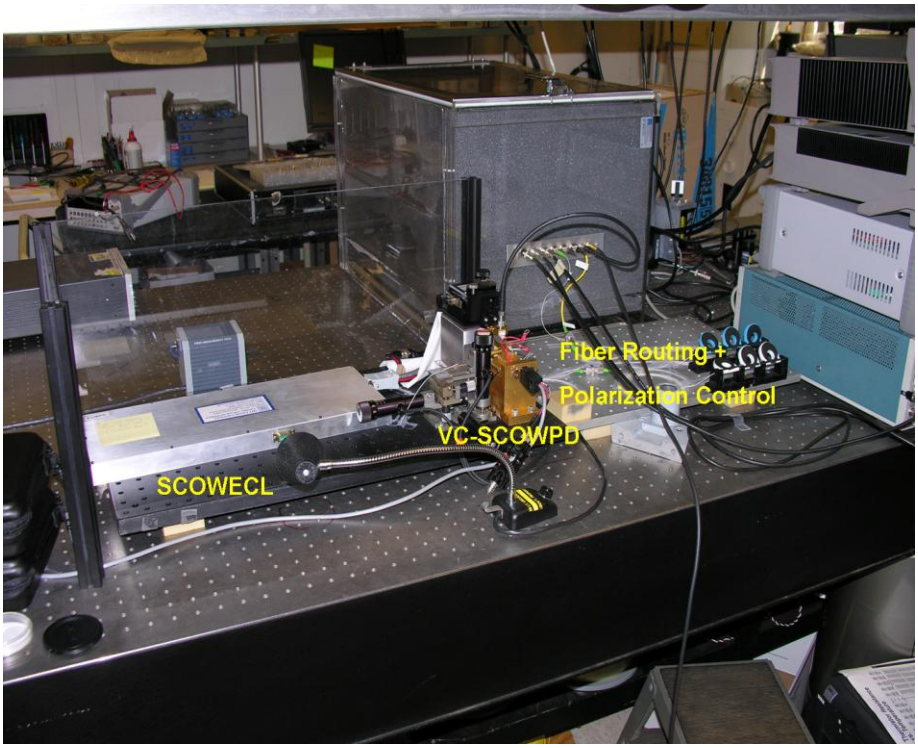

Figure 3. SCOW-OEO active component isolation box.

modulator. In addition, the RF directional coupler and modulator are housed in the box but are hidden in Figure 2. Optical and electrical interconnects are interfaced via a connector panel attached to one side of the box. The components are placed on a Thorlabs breadboard resting on top of vibration damping rubber blocks. Similar rubber blocks also support the base of the fiber spool and provide additional stability to the system. Acoustic foam and sealant was used to cover the walls of the box for encapsulation of interior components. A thermoelectric cooler (TEC) and thermistor were incorporated in order to provide temperature stabilization to the unit. The isolation box was typically operated at room temperature to prevent excess thermal loading on the heat sink. In addition, the active components were housed within a second box to further limit stress on the temperature controller.

The isolation box used for the active components (SCOWECL and VC-SCOWPD) is shown in Figure 3. The SCOWECL was packaged in a 16X6 $in.^2$ assembly unit, while the VC-SCOWPD was probed and fiber-coupled in a bench-top setup. The SCOWECL dissipates ~6 W of power at 3 A and the VC-SCOWPD dissipates ~100 mW at 27 mA photocurrent. Thermoelectric controllers were used to stabilize both the SCOWECL and VC-SCOWPD to 16 °C. The components rest on an optical breadboard supported by vibration damping rubber blocks. The rubber blocks significantly improve performance as experimentally determined phase-noise is >30 dB lower with their use. One significant contribution to the noise results from the lensed fiber interface to the VC-SCOWPD. Lensed fiber vibrations cause fluctuations in the coupling that increase the noise of the derived RF signal. The active components are enclosed in a plexiglass box that can be readily disassembled for convenient microscope access. The active and passive components within the isolation boxes are routed via fiber patch cords fixed to a separate breadboard. Fiber polarization controllers are also mounted on this assembly. The polarization

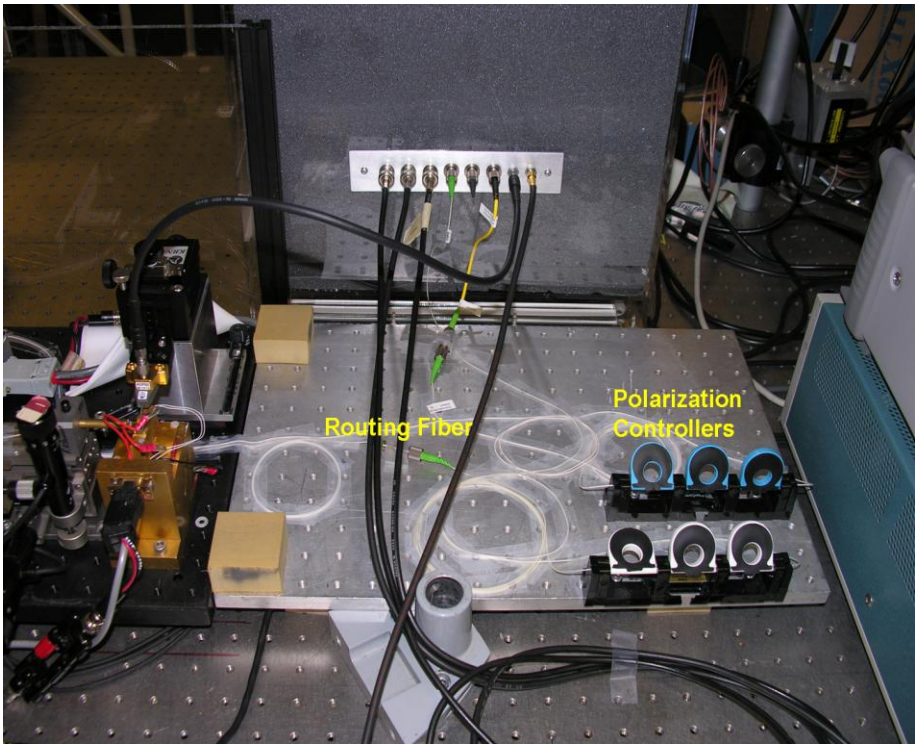

Figure 4. SCOW-OEO interconnect fibers.

controllers are required to optimize operation for the modulator and VC-SCOWPD in the OEO system. The breadboard is once again supported on rubber blocks. A close-up photograph of the interconnect assembly is shown in Figure 4.

PHOTONIC-DELAY PHASE-NOISE MEASUREMENT

The measured phase-noise of our SCOW-OEO was previously found to be limited over the measurement range 10 Hz – 10 MHz by the measurement floor of the Agilent E5052B SSA used. To measure the phase-noise below this floor, we constructed a photonic-delay frequency discriminator for converting phase fluctuations into a corresponding intensity signal. The frequency discriminator is convenient because it eliminates the requirement for a low noise reference source unlike other techniques for phase-noise measurement. A delay line converts frequency noise into a phase shift, which is later converted into a corresponding intensity beat note. We follow Yao **[15]** and Zhou **[16]** in modifying the SCOW-OEO configuration to elegantly incorporate the photonic delay line measurement, taking advantage of the modulator's second output arm. This section will detail the photonic-delay measurement system and the results of the measured phase-noise.

SCOW-OEO PHOTONIC DELAY LINE MEASUREMENT SYSTEM

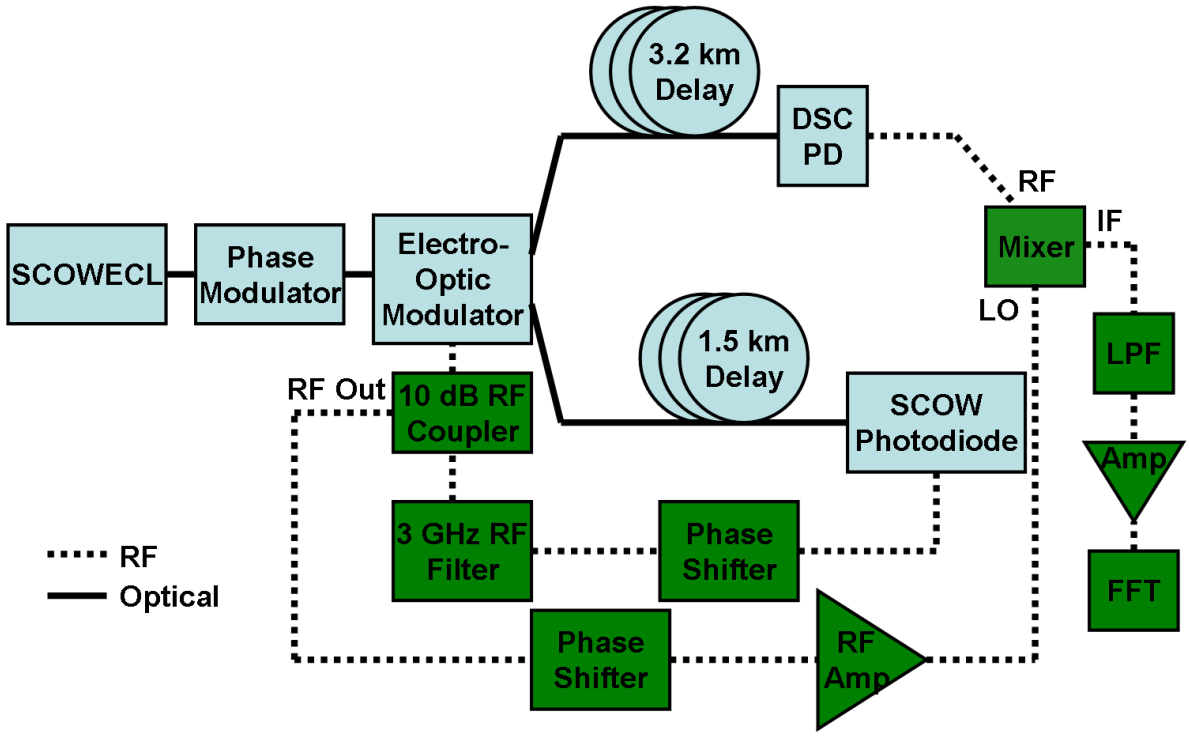

Figure 5. Schematic of SCOW-OEO incorporating both RF signal generation and photonic delay line phase-noise measurement.

The schematic of the SCOW-OEO combining both RF signal generation and phase-noise measurement is illustrated in Figure 5. The components that comprise the photonic delay phase-noise measurement system are the same as the components of the OEO. The alternate output of the EOM becomes the modulated optical carrier that is delayed by 3.2 km and photodetected before entering the mixer RF arm. A separate isolation unit houses the fiber delay used in this measurement system. The phase modulator is relocated before the modulator so that both modulated outputs can benefit from SBS noise suppression. The OEO RF output forms the reference and is sent to an RF phase shifter and amplified using a low phase-noise 2-6 GHz amplifier before entering the LO arm of the mixer. The RF amplifier employed is manufactured by AML Communications (model AML26PNC1002). The mixer output is low-pass filtered (f_C = 100 kHz) and amplified with a Stanford Research Systems SRS 560 voltage pre-amplifier before detection by an Agilent Vector Signal Analyzer. The mixer used in the measurement system has a conversion loss of 7 dB and exhibits an RF 1-dB compression power of 3 dBm with an LO drive of 7 dBm. The input powers on the RF and LO arms are ~5 dBm and ~10 dBm respectively. The photodiode used on the RF arm is a Discovery Highly-Linear Photodiode (DSC-HLPD) with saturation photocurrent ~34 mA.

To calibrate the measurement system, a voltmeter was swapped in for the FFT analyzer in the setup of Figure 5. The FFT analyzer and voltmeter input impedances are both 1 MΩ to ensure similar loading of the DC amplifier. The phase shifter is tuned until the voltmeter reads 0 V corresponding to when the mixer input arms are 90° out-of-phase. At DC, the mixer conversion of phase-to-voltage follows a dependence of $A\sin(\Delta\theta)$ when the phase between the two arms ($\Delta\theta$) is varied. The conversion slope (K_φ) is then proportional to $A\cos(\Delta\theta)$ where the two arms are initially out-of-phase when $\Delta\theta = 0$. Assuming small phase offsets (reasonable for a low phase-noise oscillator), the conversion slope is simply the amplitude (A) of the heterodyne beat note. We determine this amplitude by tuning the two arms to be completely in-phase and recording the value of the voltage measured on the voltmeter.

SCOW-OEO PHOTONIC DELAY LINE MEASUREMENT

The single-sideband (SSB) phase-noise measured of our SCOW-OEO system using the photonic-delay technique is shown in Figure 6. The length of the photonic-delay used was 3.2 km. In the figure, we have also provided the SCOW-OEO phase-noise measured by the Agilent SSA along with the specified SSA noise floor. The operating conditions were 2.5 A bias for the SCOWECL and 35 mA photocurrent for the VC-SCOWPD. Note that these differ from the I_{BIAS} = 3.0 A and I_{PD} = 27 mA operating conditions used in Reference **[6]**. In this work, we operated the modulator in quadrature to achieve higher gain while simultaneously reducing the photocurrent load on the DSC-HLPD.

The agreement between the SSA and the photonic delay line technique is excellent below 3 kHz. Between 3 kHz and 700 kHz, the SSA phase-noise is clamped by the noise floor of the system. Past ~781.3 kHz, the resolution bandwidth of the SSA increases from 3.1 kHz to 25 kHz. The large bandwidth integrates over harmonics of the 60 kHz phase modulation spurs and can easily skip the nulls between peaks due to the >15 kHz sampling point spacing. This can be visually verified through the blurring of nulls and peaks past ~800 kHz in the spectrum of Figure 6. Beyond ~2 MHz, the phase-noise drops sharply due to the influence of the RF filter. The photonic delay-line measurement was truncated at 43 kHz to eliminate corruption near the frequency where the phase wraps around to 2π **[7]**.

At low frequencies (<1 kHz), the noise peaks are due to a combination of 60 Hz line noise and photodiode noise. The measured SCOW-OEO phase-noise is -143 dBc/Hz at 10 kHz offset and reaches a minimum of -153 dBc/Hz at the last data point (43 kHz) of the photonic-delay measurement. At 10 Hz, 100 Hz, and 1 kHz, the phase-noise is -50 dBc/Hz, -80 dBc/Hz, and -115 dBc/Hz, respectively. These

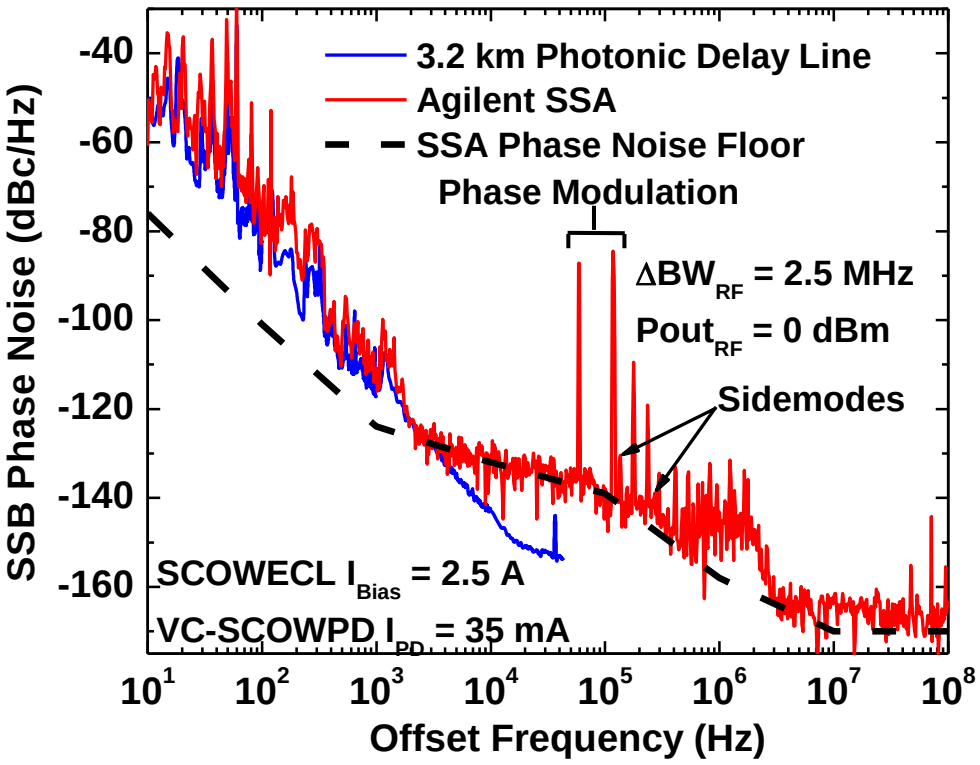

Figure 6. Comparison of single-sideband (SSB) phase-noise measured using the Agilent SSA and the photonic delay line technique. Noise floor of the SSA also shown.

values are significantly higher than those measured in Reference **[6]**. The degradation in phase-noise arises from noise processes in the photodiode, as will be illustrated in the next section.

VC-SCOWPD AMPLITUDE AND PHASE RESPONSE

Photodiode noise in an OEO results from conversion of the laser amplitude noise into electrical phase-noise (AM_o-PM_e) and amplitude noise (AM_o-AM_e) **[13]**. The amplitude noise becomes the effective RIN of the electrical signal, while the amplitude-to-phase noise conversion results in a broadening of the OEO RF spectrum. These noise processes change as a function of photocurrent because charge screening affects the speed of the electron transport and the resulting RF power. Here, we measure the VC-SCOWPD AM_o-AM_e and AM_o-PM_e noise by performing S21 measurements on the VC-SCOWPD. The RF modulation power was 5 dBm to maintain similar operating conditions compared to the OEO operation (10 dBm on a 2.8 V_π EOM). Operation under the exact power and modulator conditions is not important. The only requirement is that the modulation power is large-signal compared to the intensity-noise processes of the laser.

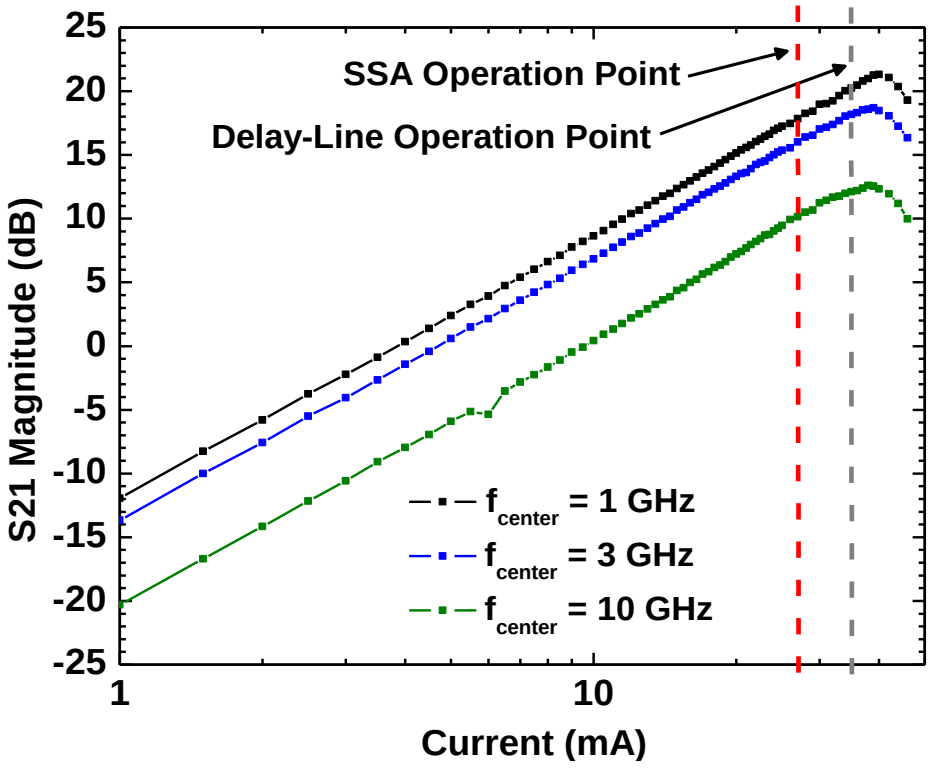

Figure 7. VC-SCOWPD S21 magnitude response at 1, 3, and 10 GHz.

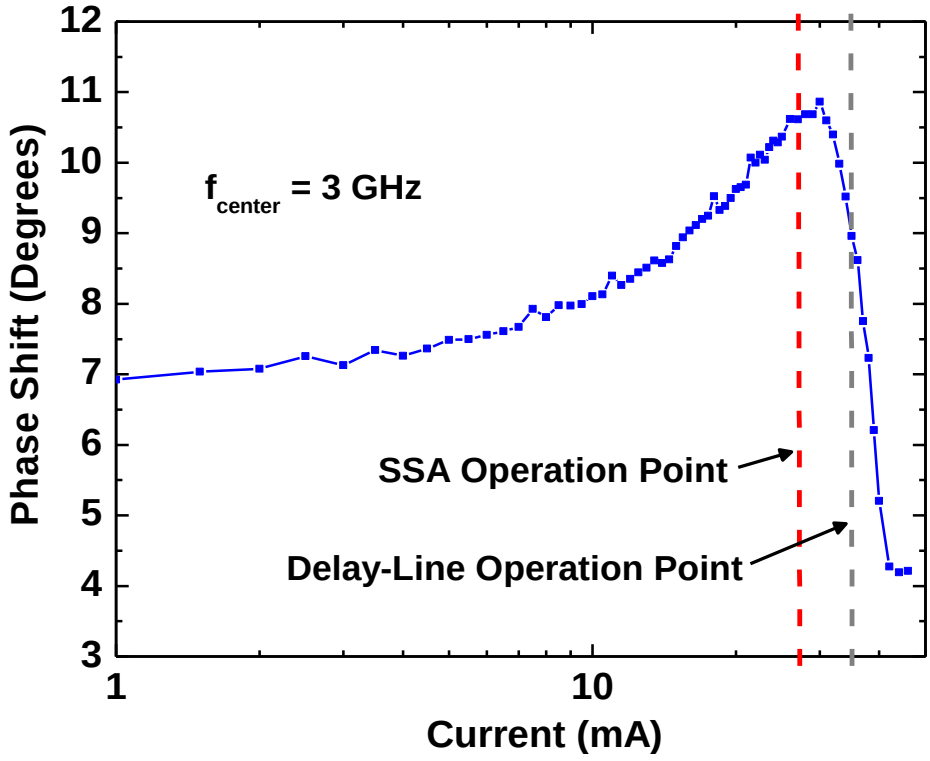

Figure 8. 3 GHz VC-SCOWPD S21 phase response.

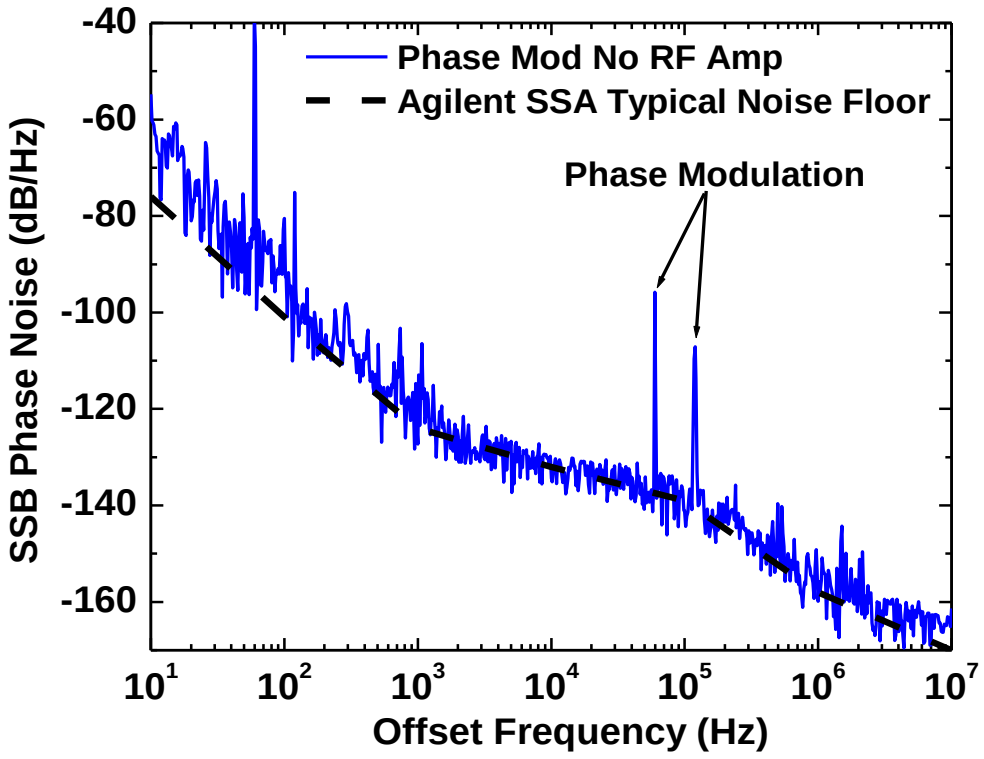

Figure 9. Measured 3 GHz SCOW-OEO SSB phase-noise spectrum of Ref. **[6]**.

The S21 magnitude and phase measurements for the VC-SCOWPD are shown in Figures 7 and 8. The red and gray dashed lines respectively indicate the photocurrent operation regimes for the SSA measurement in Ref. **[6]** and the photonic-delay measurement reported here. The ideal photocurrent operating point for both graphs occurs at the zero-slope point where charge saturation stabilizes the RF amplitude and phase against fluctuations in current. Unfortunately, the zero-slope points in amplitude and phase do not coincide at the same current. For the operating conditions of the SCOWPD shown, it is not possible to simultaneously achieve suppression of both amplitude and phase-noise. Our experimentally optimized SCOW-OEO operation in Ref. **[6]** revealed that suppression of the AM_o-PM_e noise is critical for low phase-noise. The phase-noise of the SCOW-OEO measured in Ref. **[6]** is provided in Figure 9 for comparison.

The gray dashed line in Figure 8 indicates that the operation point of the SCOW-OEO during the photonic-delay phase-noise measurements did not coincide with either of the amplitude or phase zero-slope points. Operation at ~27 mA was not possible as the threshold for oscillation under quadrature-bias conditions was > 30 mA. The optoelectronic gain can be increased if the laser bias is simultaneously increased as the modulator is low-biased. This procedure was used for the SCOW-OEO demonstration in Ref. **[6]**. However, this technique greatly increases the optical` power (~100 mW) incident on the DSC-HLPD via the second modulator arm. Optical attenuation (3 dB) would be required to mitigate photodiode saturation but would result in ~6 dB attenuation in RF power. This greatly reduces the sensitivity of the mixer for phase-detection.

In our system, photodiode AM_o-PM_e adds the largest contribution to phase-noise as the SCOWECL RIN is already low. Thus, increasing the photocurrent to the RIN suppression point would not provide any benefits if the AM_o-PM_e noise is not correspondingly reduced. As evident from the previous discussion, the degradation in phase-noise measured in Figure 6 is due to the photodiode AM_o-PM_e noise process.

SCOW- COUPLED OPTOELECTRONIC OSCILLATOR

A coupled optoelectronic oscillator (COEO) can be constructed by slightly modifying the configuration of the OEO **[8,17]**. A schematic of our SCOW-COEO is shown in Figure 10. In the optical loop, the SCOW-COEO consists of a high-power (P_{sat} ~ 500 mW) high-gain (G_o~30 dB) SCOW amplifier (SCOWA), ~250 m of fiber delay, and an EOM having V_π=2.9 V and loss=2.5 dB. The FSR of the optical loop is 765 kHz. Using a 90:10 splitter, we couple 10% of the light out into a Discovery DSC50S photodiode (PD). The resulting electrical signal is amplified by a low phase-noise RF amplifier (G_e~14 dB) before being sent to a 10 GHz RF filter with ~10 MHz bandwidth. An RF directional coupler couples out 10% of the RF signal as useful output before feeding the signal back into the modulator for self-oscillation.

The phase-noise of the RF output was measured using the Agilent SSA system. The RF power output from the 10 dB coupler was close to 0 dBm. Figure 11 shows the single-sideband phase-noise measured

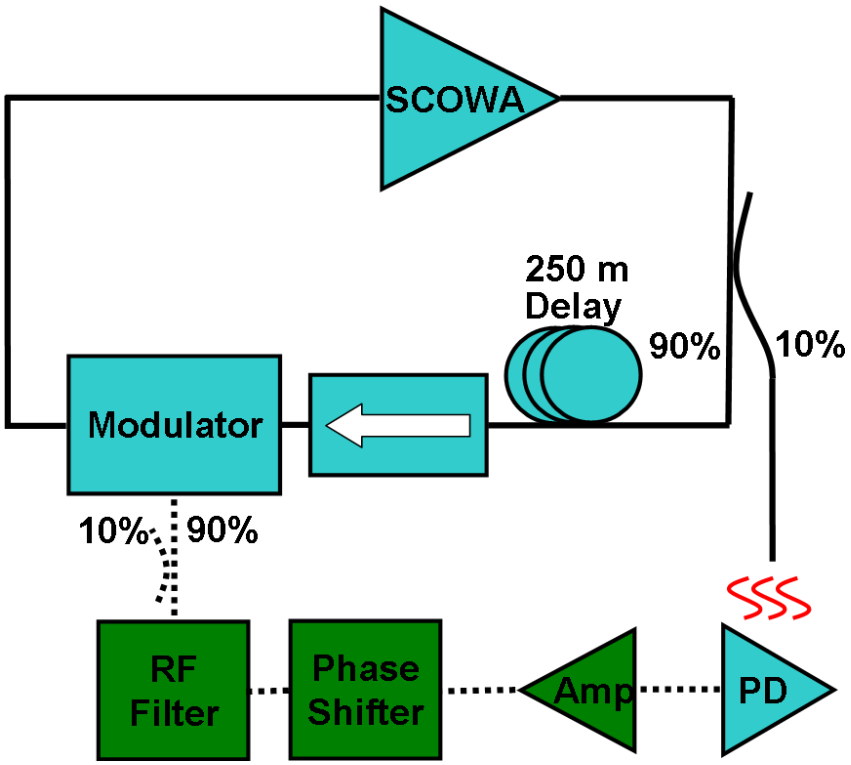

Figure 10. Configuration of a high-performance SCOW-COEO.

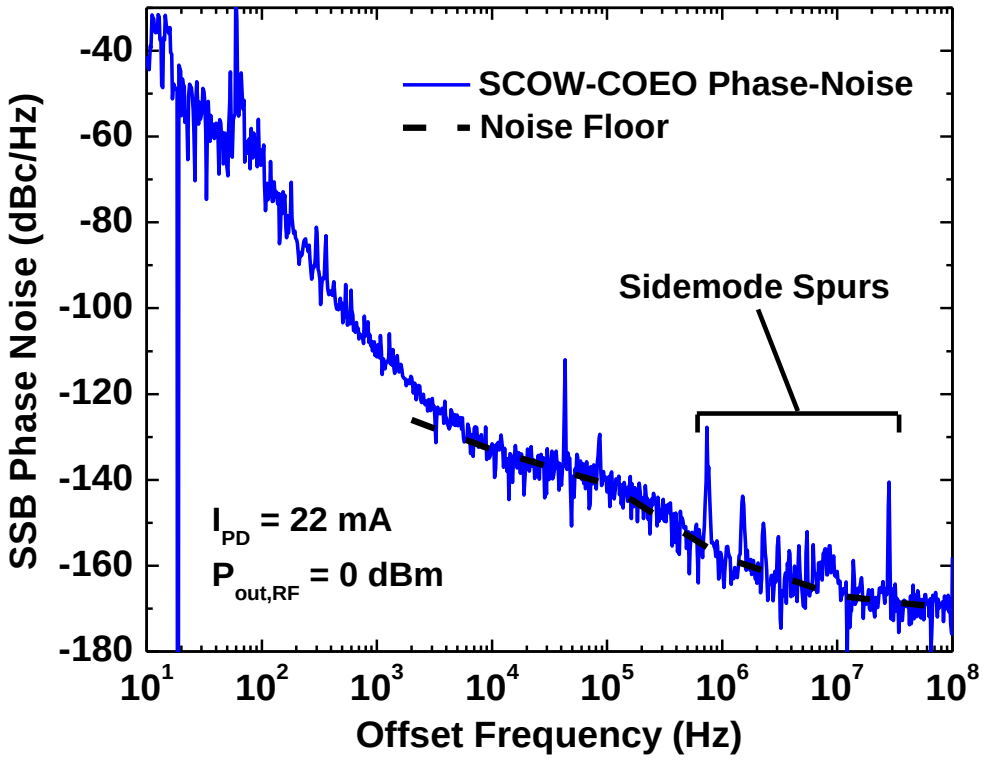

Figure 11. 10 GHz SCOW-COEO single-sideband (SSB) phase-noise.

using the Agilent SSA. The noise floor of the measurement is also provided, determined through cross-correlation measurements on a separate low-noise 10 GHz oscillator.

The phase-noise of the SCOW-COEO is -40 dBc/Hz, -70 dBc/Hz, -110 dBc/Hz, and -134 dBc/Hz at 10 Hz, 100 Hz, 1 kHz, and 10 kHz offset frequencies, respectively. The sidemode levels are <-127 dBc/Hz with an RF filter bandwidth of 10 MHz. The integration bandwidth of the SSA near 7-10 MHz offset frequency averages over multiple sidemodes and causes the phase-noise to exhibit a broad peak. Finally, the sidemode at ~28 MHz is the next frequency resonant in both the optical and electrical cavities. The gain of this mode is severely weakened by the cutoff of the filter, thereby suppressing its oscillation. The measured phase-noise is slightly worse than that of the best COEOs reported in the literature **[10,17]**. Further optimization is needed to improve the performance of the SCOW-COEO system. The average circulating intracavity optical power of the pulses was ~270 mW. Currently, no additional characterization has been conducted regarding the performance of the optical pulse train. The measurements of the optical pulses will be detailed in a future publication.

CONCLUSION

A SCOW-OEO system has been demonstrated using a high-power low-noise SCOWECL and a high-power VC-SCOWPD. The OEO can be modified to a photonic-delay phase-noise measurement system

capable of simultaneously generating and measuring a pristine microwave signal. The phase-noise performance of the SCOW-OEO was -143 dBc/Hz at 10 kHz offset and reaches a minimum of -153 dBc/Hz at the last data point (43 kHz) of the measurement. The phase-noise of the SCOW-OEO is limited by the AM_o-AM_e photodiode noise process. We have also demonstrated an initial SCOW-COEO system comprising a high-power high-gain SCOWA with a commercial Discovery photodiode. The measured SCOW-COEO phase-noise was -134 dBc/Hz at 10 kHz offset. We expect that optimization of the configuration will result in further improvements to the SCOW-COEO performance.

REFERENCES

[1] R. C. Taber and C. A. Flory, 1995, *"Microwave oscillators incorporating cryogenic sapphire dielectric resonators,"* **IEEE Trans. Ultrasonics, Ferroelect., Freq. Contr., Vol. 42**, 111-119.

[2] X. S. Yao and L. Maleki, 1996, *"Optoelectronic oscillator for photonic systems,"* **IEEE J. Quantum Electron., Vol. 32**, 1141-1149.

[3] X. S. Yao and L. Maleki, 1996, *"Optoelectronic oscillator microwave oscillator,"* **J. Opt. Soc. Am. B, Vol. 13**, 1725-1735.

[4] D. Eliyahu and L. Maleki, 2003, *"Low phase noise and spurious levels in multi-loop opto-electronic oscillators,"* in Proc. IEEE Freq. Control Symp., pp. 405-410.

[5] W. Zhou and G. Blasche, 2005, *"Injection-locked dual opto-electronic oscillator with ultra-low phase noise and ultra-low spurious level,"* **IEEE Trans. Microwave Theory Tech., Vol. 53**, 929-933.

[6] W. Loh, J. Klamkin, S. M. Madison, F. J. O'Donnell, J. J. Plant, S. Yegnanarayanan, R. J. Ram, and P. W. Juodawlkis, 2011, *"Slab-Coupled Optical Waveguide (SCOW) based Optoelectronic Oscillator (OEO),"* in Proc. IEEE Photonics Conference (IPC).

[7] E. Rubiola, E. Salik, S. Huang, N. Yu, and L. Maleki, 2005, *"Photonic-delay technique for phase-noise measurement of microwave oscillators,"* **J. Opt. Soc. Am. B, Vol. 22**, 987-997.

[8] X. S. Yao and L. Maleki, 1997, *"Dual microwave and optical oscillator,"* **Opt. Lett., Vol. 22**, 1867-1869.

[9] M. Nakazawa, E. Yoshida, and Y. Kimura, 1994, *"Ultrastable harmonically and regeneratively modelocked polarization-maintaining erbium fibre ring laser,"* **Electron. Lett., Vol. 30**, 1603-1605.

[10] D. Eliyahu and L. Maleki, 2005, *"Modulation response (S21) of the coupled opto-electronic oscillator,"* in Proc. IEEE Freq. Control Symp., pp. 850-856.

[11] W. Loh, J. J. Plant, J. Klamkin, J. P. Donnelly, F. J. O'Donnell, R. J. Ram, and P. W. Juodawlkis, 2011, *"Noise Figure of Watt-Class Ultralow-Confinement Semiconductor Optical Amplifiers,"* **IEEE J. Quantum Electron., Vol. 47**, 66-75.

[12] J. Klamkin, S. M. Madison, D. C. Oakley, A. Napoleone, F. J O'Donnell, M. Sheehan, L. J. Missaggia, J. M. Caissie, J. J. Plant, and P. W. Juodawlkis, 2011, *"Uni-Traveling-Carrier Variable Confinement Waveguide Photodiodes,"* **Opt. Express**.

[14] C. W. Nelson, A. Hati, and D. A. Howe, 2008, *"Relative Intensity Noise Suppression for RF Photonic Links,"* **IEEE Photon. Technol. Lett., Vol. 20**, 1542-1544.

[15] X. S. Yao, 2002, *"Opto-electronic Oscillators,"* in **RF Photonic Technology in Optical Fiber Links,** W. S. C. Chang, Ed.: Cambridge University Press, PP. 255-292.

[16] W. Zhou, 2008, *"10 GHz dual loop opto-electronic oscillator without RF-amplifiers,"* **Proc. SPIE, Vol. 6897**, p. 68970Z.

[17] D. Eliyahu, D. Seidel, and L. Maleki, 2008, *"Low phase noise and spurious levels in multi-loop opto-electronic oscillators,"* in Proc. IEEE Freq. Control Symp., pp. 811-814.